Pergamon

PII: S0148-9062(97)00316-1

Int. J. Rock Mech. Min. Sci. Vol. 35, No. 1, pp. 69–74, 1998

Printed in Great Britain
0148-9062/98 $19.00 + 0.00

Technical note

2-D BEM Analysis of Anisotropic Half-plane Problems—application to Rock Mechanics

E. PAN†
B. AMADEI†
Y. I. KIM‡

INTRODUCTION

Many problems in engineering and geosciences require models associated with a half-plane domain. Examples can be found in rock engineering related to underground or surface excavations, and in geophysics when estimating analytically the regional *in situ* stresses in the Earth.

Previously, several analytical and numerical methods have been proposed for the study of half-plane related problems. The analytical methods include the bipolar coordinates transformation [1–3], the perturbation approach [4–7], the exact conformal mapping method [8, 9], and the semi-analytical conformal mapping technique [10, 11]. Since analytical methods are restricted to simple problems only [12], numerical methods need to be used for half-plane problems with complex geometries and boundary conditions. Applications of the finite element method (FEM) to half-plane problems were presented by Zienkiewicz *et al.* [13], Barla [14] and Soliman *et al.* [15]. The FEM is applied to a finite domain which is truncated from the infinite plane. This truncation may introduce errors to the solution. Applications of boundary element method (BEM) related methods to some specific half-plane problems were conducted by various authors [16–20] who used the Kelvin-type Green's functions in their formulae. This approach requires the introduction and discretization of a fictitious outer boundary. Therefore, in the modeling of half-plane problems, the best approach would be a BEM formulation with Green's functions that does not require the introduction of fictitious outer boundaries.

Complete Green's functions for an isotropic half-plane were used by Telles and Brebbia [21] and Meek and Dai [22] in their BEM formulation. Green's functions and boundary integral equations were derived by Dumir and Mehta [23] for orthotropic half-plane problems. Recently, the authors [12] obtained complete Green's functions and proposed a BEM formulation for generalized anisotropic half-plane problems.

This note is part of continuing research on the applications of BEM to rock mechanics problems. In this note, the BEM formulation for generalized anisotropic half-planes is first presented. The complete Green's functions in such domain are then summarized. Finally, two examples of application of the proposed method to rock engineering problems are presented. One deals with the distribution of gravity-induced stresses along the boundary of two adjacent tunnels in anisotropic ground. The other example illustrates the effect of anisotropy on the principal stress distribution induced by gravity and a uniform pressure applied at the surface of a rock mass.

BEM FORMULATION FOR 2-D ANISOTROPIC MEDIA

Following the procedure outlined by Pan and Amadei [24, 25], one can derive the following boundary integral equation for a 2-D anisotropic linearly elastic continuum with boundary S subjected to the body force of gravity and/or far-field stresses

$$b_{ij}u_j^l(\mathbf{Y}_S) + \int_S T_{ij}^*(\mathbf{Y}_S, \mathbf{X}_S)u_j^l(\mathbf{X}_S)\,dS(\mathbf{X}_S) = \int_S U_{ij}^*(\mathbf{Y}_S, \mathbf{X}_S)T_j^t(\mathbf{X}_S)\,dS(\mathbf{X}_S) + \int_S T_{ij}^*(\mathbf{Y}_S, \mathbf{X}_S)(u_j^p(\mathbf{X}_S) - u_i^p(\mathbf{Y}_S))\,dS(\mathbf{X}_S) - \int_S U_{ij}^*(\mathbf{Y}_S, \mathbf{X}_S)T_j^p(\mathbf{X}_S)\,dS(\mathbf{X}_S) \quad (1)$$

where the superscript t denotes the total solution, and p a particular solution corresponding to the body forces and/or the far-field stresses; $\mathbf{X}_S$ and $\mathbf{Y}_S$ are two points on the boundary S; b_{ij} are coefficients that depend only upon the local geometry of the boundary at $\mathbf{Y}_S$; dS is a line element on the boundary; and U_{ij}^* and T_{ij}^* are the Green's displacements and tractions which will be presented in the next section.

†Dept. of Civil Engineering, University of Colorado, Boulder, CO 80308, U.S.A.
‡Daewoo Institute of Construction Technology. Suwon, Korea.

It is noted that all the terms on the right-hand side of Equation (1) have only weak singularities, thus, are integrable. Although the second term on the left-hand side of Equation (1) has a strong singularity, it can be treated by the rigid-body motion method. At the same time, the calculation of b_{ij}, which is geometry dependent, can also be avoided. It is noteworthy that in Equation (1), the effect of the body force of gravity and/or the far-field stresses has been included by superposition of the corresponding particular solutions, which makes the problem very similar to the one associated with the homogeneous equations except that for the body force and/or far-field stress cases, two extra integral terms related to the particular solutions are added to the integral Equation (1). Thus, the method which consists of artificially truncating the infinite domain [26] or the method which consists of transferring the far-field stresses onto the boundary (or opening) of the problem [21, 23] can be avoided. It is apparent that the former method introduces errors and increases the size of the problem because of the truncation of the region, and the latter may not be suitable for cases where the boundaries or openings have complex shapes.

The boundary integral Equation (1) can be discretized and solved numerically for the unknown boundary displacements and tractions. Once the boundary problem is solved, the internal displacements can be found by an integral equation similar to Equation (1) [24, 25]. Furthermore, with the solved boundary displacements and tractions, the boundary stresses can also be obtained [27]. In order to calculate the internal stresses, the derivative of the internal displacement with respect to the internal coordinates $\mathbf{X}_p$ needs to be taken. This procedure results in the following integral equation [24, 25]:

$$u^{I}_{i,k}(\mathbf{X}_p) + \int_S T^{*}_{ij,k}(\mathbf{X}_p, \mathbf{X}_S) u^{I}_j(\mathbf{X}_S)\, dS(\mathbf{X}_S)$$
$$= u^{p}_{i,k}(\mathbf{X}_p) + \int_S U^{*}_{ij,k}(\mathbf{X}_p, \mathbf{X}_S) T^{I}_j(\mathbf{X}_S)\, dS(\mathbf{X}_S)$$
$$+ \int_S T^{*}_{ij,k}(\mathbf{X}_p, \mathbf{X}_S) u^{p}_j(\mathbf{X}_S)\, dS(\mathbf{X}_S)$$
$$- \int_S U^{*}_{ij,k}(\mathbf{X}_p, \mathbf{X}_S) T^{p}_j(\mathbf{X}_S)\, dS(\mathbf{X}_S) \qquad (2)$$

Once the $u^{I}_{i,k}$ are obtained, the known constitutive relation can then be used to calculate the internal stresses. It is noteworthy that in Equations (1) and (2), the Green's displacements and stresses and the particular solutions of displacements and stresses (tractions) need to be provided. While the particular solutions corresponding to the body force of gravity and to the far-field stresses can be easily obtained [12, 28], the exact closed-form solutions for the Green's functions in an anistropic half-plane are more complicated. They were derived recently by the authors [12], and are summarized in the next section.

GREEN'S FUNCTIONS FOR ANISOTROPIC HALF-PLANES

Green's functions for anisotropic solids in an infinite plane have been studied by several authors, notably by Eshelby *et al.* [29], Stroh [30] and Lekhnitskii [31]. For an anisotropic half-plane, Green's functions were studied by Suo [32] using the one-complex function method, and by Ting and co-workers [33–35] based on the Stroh tensor method. In this note the one-complex function method introduced by Suo [32] is followed.

In general, by using three complex functions $f_i(z_i)$, the displacement and stress fields in an anisotropic medium can be expressed as [10, 31, 32]

$$u_i = 2\ \mathrm{Re}\left[\sum_{j=1}^{3} A_{ij} f_j(z_j)\right]$$
$$\sigma_{2i} = 2\ \mathrm{Re}\left[\sum_{j=1}^{3} L_{ij} f'_j(z_j)\right]$$
$$\sigma_{1i} = -2\ \mathrm{Re}\left[\sum_{j=1}^{3} L_{ij}\, \mu_j f'_j(z_j)\right] \qquad (3)$$

where a prime denotes the differentiation; Re denotes the real part of a complex variable or function; $z_j = x + \mu_j y$ with (x, y) being the Cartesian coordinates of the field point; and the complex roots μ_j (j = 1,2,3) and the elements of the complex matrices [**L**] and [**A**] all depend on the material properties. Their expressions can be found in Lekhnitskii [31], Suo [32] or Pan and Amadei [10].

For concentrated forces acting at the source point (x^0, y^0), the complex functions in Equation (3) can be expressed as [25, 32]

$$f_j(z_j) = \sum_{k=1}^{3} \frac{-1}{2\pi} D_{jk}\, P_k \ln(z_j - z^0_j) \qquad (4)$$

In Equation (4), $z^0_j = x^0 + \mu_j y^0$, P_k (k = 1,2,3) is the magnitude of the point force in the k-direction; and the elements of the complex matrix [**D**] are given in Pan and Amadei [25]. The substitution of the complex functions [Equation (4)] into Equation (3) gives the Green's displacements and stresses in an anisotropic infinite-plane [24].

For an anisotropic half-plane, let the medium occupy the lower half-plane ($y < 0$) and let $y = 0$ correspond to the traction-free surface. To find the complex functions in Equation (3), add to the complex function [Equation (4)] a complementary part such that the traction-free condition at $y = 0$ is enforced. This procedure involves the analytical continuation of complex functions. Following this path and after some complex algebraic manipulation, the complementary part of the function can be found. Substituting the solved complex function into Equation (3), the Green's functions corresponding to the half-plane domain are obtained. For displacements, these Green's functions are

$$U^*_{kl} = \frac{-1}{\pi}\mathrm{Re}\left\{\sum_{j=1}^{3} A_{lj}\left[D_{jk}\ln(z_j - z_j^0) - \sum_{i=1}^{3} E_{ji}\bar{D}_{ik}\ln(z_j - \bar{z}_i^0)\right]\right\} \quad (5)$$

and for tractions, they are

$$T^*_{kl} = \frac{1}{\pi}\mathrm{Re}\left\{\sum_{j=1}^{3} L_{lj}\left[\frac{\mu_j n_x - n_y}{z_j - z_j^0} D_{jk} - \sum_{i=1}^{3} E_{ji}\frac{\mu_j n_x - n_y}{z_j - \bar{z}_i^0}\bar{D}_{ik}\right]\right\} \quad (6)$$

In Equations (5) and (6), a bar over a quantity denotes the complex conjugate; the matrix [**E**] is related to the anisotropic elastic properties [12]; and n_x and n_y are the outward normal components of the field point z_j. For the calculation of internal stresses, the derivative of the above Green's functions with respect to the source point z_i^0 is needed and this can be easily done.

It is noteworthy that the first terms on the right-hand side of Equations (5) and (6) are actually the Green's functions for an anisotropic infinite plane. Therefore, Equations (5) and (6) can be used for problems dealing with finite, infinite and semi-infinite domains.

NUMERICAL EXAMPLES

The aforementioned Green's functions have been incorporated into the boundary integral Equation (1), and the results have been programmed. The program has been tested by the authors [12] for various problems (dealing with isotropic media) for which analytical solutions are available. Two examples of applications of the new BEM formulation to rock engineering problems are presented below.

The first example deals with the stress distribution around two underground openings in anisotropic ground. Figure 1 shows the geometry of two tunnels located at a finite depth, R, below the surface of an anisotropic rock mass. A total of 25 quadratic elements with a total of 54 nodes were used to discretize the boundary of each tunnel. Since the half-plane Green's functions have been incorporated into our BEM program, no discretization was required along the ground surface. The rock mass is transversely isotropic (layered) with its layers inclined with a dip angle ψ (0, 45 or 90°) to the $+x$ direction of Fig. 1. The elastic constants are such that $E/E' = 1/3,1$ or 3, $\nu = \nu' = 0.25$ and $G' = 0.4$ where E and E' are Young's moduli in the plane of transverse isotropy and in the direction normal to it, respectively; ν and ν' are Poisson's ratios characterizing the lateral strain response in the plane of transverse isotropy to a stress acting parallel and normal to it, respectively; and G' is the shear modulus in planes normal to the plane of transverse isotropy. The normalized tangential (hoop) stress ($\sigma_{\theta\theta}/2\rho gR$ along the roof AB, $\sigma_{yy}/2\rho gR$ along the vertical walls BC and DA, and $\sigma_{xx}/2\rho gR$ along the horizontal floor (CD) is plotted in Fig. 2(a– d) (tension being positive). Figure 2(a and b) shows the stress variations when the dip angle $\psi = 0°$ (horizontal rock layers) and 90° (vertical rock layers), respectively, and Fig. 2(c and d) shows the stresses for the left- and right-hand side tunnels, respectively, when the dip angle ψ is equal to 45°. In each figure, the Young's moduli ratio E/E' is equal to 1/3,1 or 3. Each figure indicates clearly that the degree of rock anistropy (represented here by the ratio E/E') has a great effect on the stress distribution. For example, it is observed from these figures that for the isotropic case ($E/E' = 1$), tensile stresses (i.e. positive stresses) develop along the roof AB and floor CD. For anisotropic rock masses with $E/E' = 3$, however, the tensile stresses

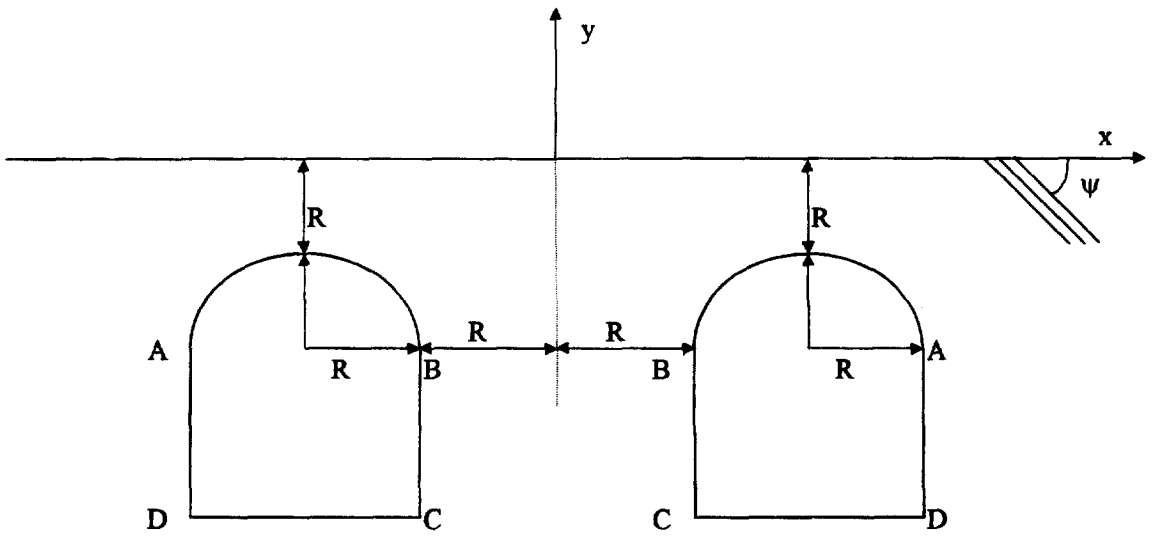

Fig. 1. Geometry of two tunnels within a half-plane of anisotropic rock mass.

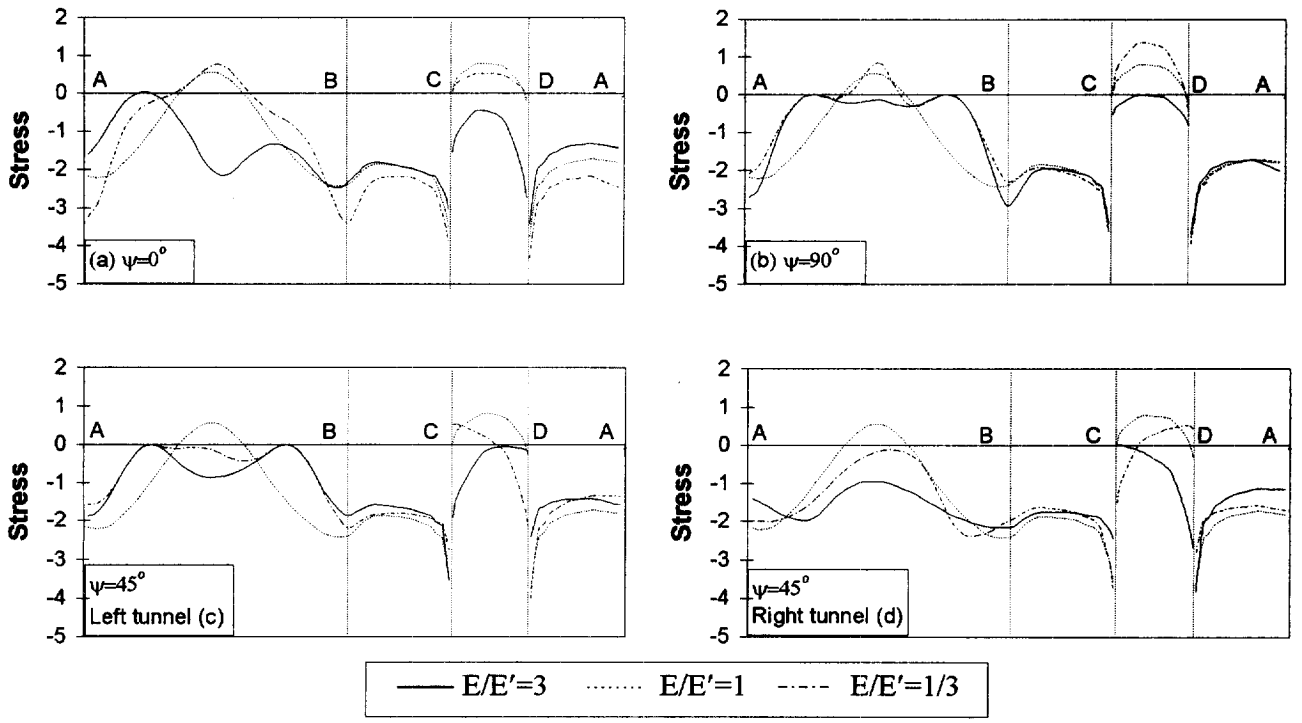

Fig. 2. Variation of the normalized hoop stress ($\sigma_{\theta\theta}/2\rho gR$ or $\sigma_{yy}/2\rho gR$ or $\sigma_{xx}/2\rho gR$) along the boundary of the tunnels, induced by the body force of gravity ρg. The dip angle ψ is: (a) 0°; (b) 90°; (c) 45° for the left-hand side tunnel and (d) 45° for the right-hand side tunnel.

vanish and are replaced by compressive stresses, the magnitude of which depends largely on the value of the dip angle ψ. The effect of the orientation of the rock layers (i.e. the dip angle ψ) on the stress distribution can also be noticed from these figures. For instance, Fig. 2(a and b) show that for $E/E' = 3$, larger compressive stress develop along the floor CD for rock masses with horizontal layers ($\psi = 0°$) than for rock masses with vertical layers ($\psi = 90°$). Furthermore, when the rock layers are inclined (here, $\psi = 45°$), the stress distribution along the wall of the left-hand side tunnel is quite different from that along the wall of the right-hand side tunnel [see Fig. 2(c and d)].

The second example deals with the stresses induced in an anisotropic rock mass by a combination of uniform surface pressure applied over a strip area and the body force of gravity. The uniform pressure p is applied over the interval $-0.5 \leq x \leq 0.5$ on the ground surface (Fig. 3). In this case, only the loaded part of the ground surface needs to be discretized. This was done using ten quadratic elements with a total of 21 nodes. The elastic constants in this example are: $E/E' = 3$, $\nu = \nu' = 0.25$ and $G' = 0.4$, while the dip angle of the rock layers ψ is equal to 0, 30, 60 or 90° (in the $+x$ direction). Figure 3(a–d) show contours of the normalized principal stress σ_1/p induced by the surface pressure p only for $\psi = 0$, 30, 60 and 90°, respectively. It is interesting to note from these figures that the stress contours tend to stretch along the direction of the dip angle. Figure 3(e–h) show similar contours of the principal stress σ_1/p induced by the surface pressure p and the body force of gravity ($\rho g = p$). It is clear that the principal stress distribution is mostly controlled by the body force of gravity except, maybe, for the region near the surface loading area.

CONCLUSION

A general 2-D BEM formulation for the analysis of half-plane problems representing anisotropic rock masses has been presented. The corresponding program can be used to model the effect of gravity and/or far-field stresses, and for problems with or without boundary tractions on the flat surface of the half-plane or along the surface openings. Since the Green's functions for a half-plane into the 2-D BEM code have been implemented, very accurate results have been obtained with relatively coarse discretizations. For half-plane problems without surface traction (i.e. the first numerical example), no discretization along the flat surface of the half-plane is necessary. For problems with surface traction (i.e. the second numerical example), only the loaded region along the flat surface needs to be discretized. Numerical applications to rock mechanics examples with the 2-D BEM program shown clearly that the degree of rock anisotropy and the orientation of the anisotropy can have a great effect on the stress distributions in rock masses. This conclusion should be considered within the context of rock engineering practice and in particular when

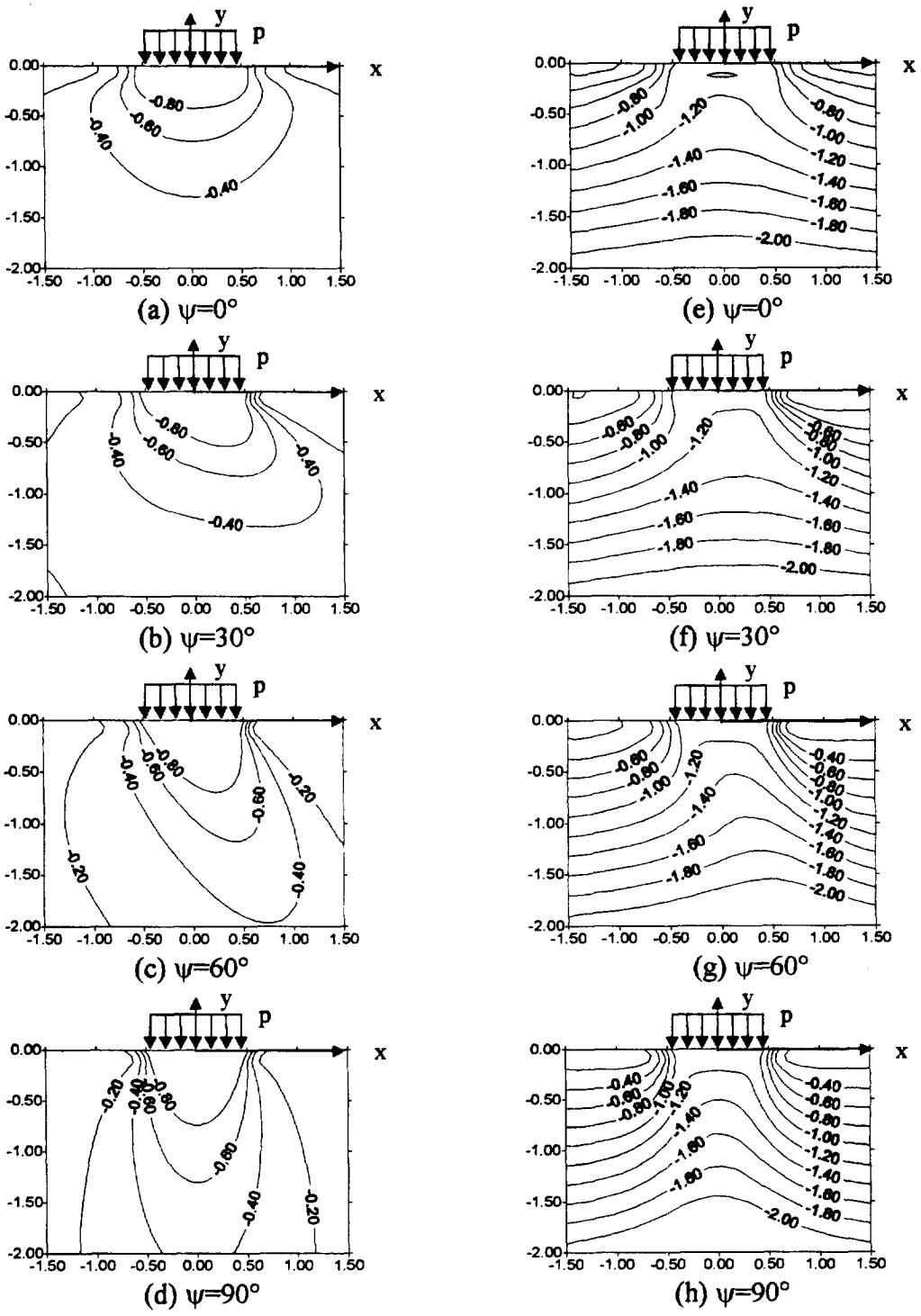

Fig. 3. Variation of the normalized principal stress σ_1/p within the half-plane. (a–d) induced by the surface pressure p only. The dip angle ψ is (a) 0°; (b) 30°; (c) 60°; and (d) 90°; (e–h) induced by the surface pressure p and the body force of gravity ($\rho g = p$). The dip angle ψ is (a) 0°; (b) 30°; (c) 60°; and (d) 90°.

designing surface openings or underground tunnels in layered ground.

The current BEM program could also find applications in the study of rock slope stability, borehole breakout and rock fracture propagation. It can also help in the performance assessment of tunnels [36] and in the estimation of *in situ* stresses in complex environments.

Acknowledgements—This paper was made possible by the support of National Science Foundation under Grant No. CMS-9622645.

Accepted for publication 1 September 1997

REFERENCES

1. Mindlin, R. D., *Trans. ASCE*, 1940, **105**, 1117–1153.

2. Mindlin, R. D., Stress distribution around a hole near the edge of a plate under tension. *Proc. of The Society for Experimental Stress Analysis*. 1948, Vol. 5, pp. 56–68.
3. Ling, C. B., *J. Math. Phys.*, 1947, **26,** 284–289.
4. Srolovitz, D. J., *Acta Metall.*, 1989, **37,** 621–625.
5. Liao, J. J., Savage, W. Z. and Amadei, B., *J. Geophys. Res.*, 1992, **97,** 3325–3336.
6. Gao, H., *J. Mech. Phys. Solids*, 1991, **39,** 443–458.
7. Gao, H., Morphological instabilities along surfaces of anisotropic solids. In *Modern Theory of Anisotropic Elasticity and Applications*, ed. J. J. Wu, T. C. T. Ting and D. M. Barnett. SIAM, Philadelphia, 1991, pp. 139–150.
8. Savage, W. Z. and Swolfs, H. S., *J. Geophys. Res.*, 1986, **91,** 3677–3685.
9. Chiu, C. and Gao, H., *Int. J. Solids Structures*, 1993, **30,** 2983–3012.
10. Pan, E. and Amadei, B., *Acta Mech.*, 1995, **113,** 119–135.
11. Pan, E., Amadei, B. and Savage, W. Z., *Int. J. Rock Mech. Min. Sci. Geomech. Abstr.*, 1995, **32,** 201–214.
12. Pan, E., Chen, C. S. and Amadei, B., A BEM formulation for anisotropic half-plane problems. *Eng. Analy. Boundary Elements*. 1997 (in press).
13. Zienkiewicz, O. C., Cheung, Y. K. and Stagg, K. G., *J. Strain Analysis*, 1966, **1,** 172–182.
14. Barla, G., *Int. J. Rock Mech. Min. Sci. Geomech. Abstr.*, 1972, **9,** 103–126.
15. Soliman, E., Duddeck, H. and Ahrens, H., *Tunneling and Underground Space Technology*, 1993, **8,** 13–18.
16. Eissa, E. A., *Stress analysis of underground excavations in isotropic and stratified rock using the boundary element method.* Ph.D. Thesis, Imperial College of Science and Technology, London, 1980.
17. Fainstein, G., Sidi, A., Israeli, M. and Tsur-Lavie, Y., Application of boundary integral equations to the solution of stresses around a shallow circular hole. In *28th US Symp. on Rock Mech.*, 1987, pp. 745–754.
18. Carter, J. P. and Alehossein, H., *Comp. Geotech.*, 1990, **9,** 209–231.
19. Xiao, B. and Carter, J. P., *Eng. Analy. Boundary Elements*, 1993, **11,** 293–303.
20. Beer, G. and Poulsen, B. A., *Int. J. Numer. Anal. Meth. Geomech*, 1994, **18,** 417–426.
21. Telles, J. C. F. and Brebbia, C. A., *Int. J. Solids Structures*, 1981, **17,** 1149–1158.
22. Meek, J. L. and Dai, C., *Computer Meth. Appl. Mech. Eng.*, 1993, **102,** 15–27.
23. Dumir, P. C. and Mehta, A. K., *Computers & Structures*, 1987, **26,** 431–438.
24. Pan, E. and Amadei, B., *Appl. Math. Modelling*, 1996, **20,** 114–120.
25. Pan, E. and Amadei, B., *Int. J. Fracture*, 1996, **77,** 161–174.
26. Lee, J. S., *Eng. Anal. Bound Elements*, 1995, **15,** 321–328.
27. Becker, A. A., *The Boundary Element Method in Engineering. A Complete Course.* McGraw-Hill, New York, 1992.
28. Amadei, B. and Pan, E., *Int. J. Rock Mech. Min. Sci. Geomech. Abstr.*, 1992, **29,** 225–236.
29. Eshelby, J. D., Read, W. T. and Shockley, W., *Acta Metal.*, 1953, **1,** 251–259.
30. Stroh, A. N., *Philos. Mag.*, 1958, **7,** 625–646.
31. Lekhnitskii, S. G., *Theory of Elasticity of an Anisotropic Body*. Holden Day, San Francisco, 1963.
32. Suo, Z., *Proc. R. Soc. Lond.*, 1990, **A427,** 331–358.
33. Ting, T. C. T., *Q. J. Mech. Appl. Math.*, 1992, **45,** 119–139.
34. Ting, T. C. T. and Barnett, D. M., *Int. J. Solids Structures*, 1993, **30,** 313–323.
35. Wei, L. and Ting, T. C. T., *J. Elasticity*, 1994, **36,** 67–83.
36. Wong, R. C. K. and Kaiser, P. K., *ASCE J. Geotech. Eng.*, 1991, **117,** 1880–1901.